A Novel Characterization Method for Accurate Lumped Parameter Modeling of Electret Electrostatic Vibration Energy Harvesters

Armine Karami, *Student Member, IEEE*, Dimitri Galayko, *Member, IEEE*, and Philippe Basset

***Abstract*— This letter presents a new method for the characterization of electret transducers, which are typically used in electret electrostatic vibration energy harvesters (electret e-VEHs). This is the first method allowing to accurately measure the value of the equivalent voltage source representing the electret in lumped parameter models of a wide range of electret e-VEHs. An accurate value for this parameter is critical for design, analysis, and optimization, given the increasing complexity of e-VEHs electrical interfaces. Until now, there was no universal method allowing the measurement of this parameter, because of practical difficulties with some geometries, and because of charging non-uniformities. In this letter, the new method is presented, with insights on how to maximize the measurement accuracy. It is then applied to a state-of-the art MEMS electret e-VEH.**

***Index Terms*— Electrostatic vibration energy harvesting, electret, charge pumps, energy conversion.**

I. Introduction

ELECTRET electrostatic vibration energy harvesters (e-VEHs) are a promising technology to power autonomous systems [1], [2]. They are composed of a mobile mass, attached to an electret-charged transducer. The biasing of this transducer is determined by a conditioning circuit. Energy conversion occurs when the bias across the transducer results in an electrostatic force opposing the mass motion induced by an external acceleration.

In the recent years, the complexity of the available conditioning circuits has increased to optimize the harvesters performances [3]–[6]. As a result, the use of lumped parameter models of e-VEHs is becoming the sole convenient way to predict their dynamics under variable input conditions.

A convenient representation of the electret-charged transducer in lumped parameter models of e-VEHs is an equivalent constant voltage source in series with the transducer's variable capacitance [7]. This source will be referred to as the electret potential in the rest of the letter. Lumped-parameter models are expected to yield accurate predictions on the e-VEH dynamics, and to guide optimization choices in the conditioning circuit design. To do this, these models have to be parametrized accurately. In particular, the electret potential value has a critical effect on the models' predictions [8, Ch. 11]) The electret potential is difficult to define precisely at the fabrication stage. Plus, it may decrease in large time scales [9]. Hence, it is necessary to measure its value after fabrication.

Manuscript received February 17, 2017; revised March 11, 2017; accepted March 11, 2017. Date of publication March 14, 2017; date of current version April 24, 2017. The review of this letter was arranged by Editor M. Tabib-Azar. *(Corresponding author: Armine Karami.)*

A. Karami and D. Galayko are with UMR 7606, LIP6, UPMC Univ Paris 06, Sorbonne Universités, F-75005 Paris, France (e-mail: armine.karami@lip6.fr).

P. Basset is with ESYCOM, ESIEE Paris, Université Paris-Est, 93160, Noisy-le-Grand, France.

Digital Object Identifier 10.1109/LED.2017.2682232

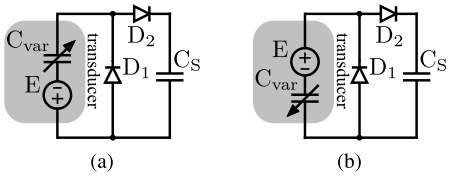

Fig. 1. Schematics of circuit HW1 (a) and circuit HW2 (b).

Until now, this was done by measuring the device's surface potential, with a contact-less electrostatic voltmeter. Ideally, this measurement has to be done between the facing capacitor plates of the transducer. However, this is impossible to perform nondestructively on a wide range of e-VEHs because of the geometry of their transducer (e.g., interdigitated-combs [10]). More importantly, this technique gives a measure of a potential which is hard to accurately relate to the value of the electret potential. In particular, its accuracy relies on the assumption of uniform charge distribution across the surfaces of the transducer's facing capacitor plates. This hypothesis is not always verified, depending on both the employed charging techniques and the transducer geometry [10], [11].

In this letter, for the first time, a non-destructive and accurate method is proposed to measure the electret potential of a given transducer. This method is compatible with a wide range of transducer geometries and charging techniques. The method is presented in Section II, with insights on how to minimize the error on the measurement. It is then applied to a state-of-the-art MEMS electret e-VEH in Section III.

II. Presentation of the Method

A. Dynamics of the Measurement Circuits

The measurement method presented in this letter is based on the dynamics of the half-wave circuits HW1 and HW2, depicted in Fig. 1a and 1b, respectively. In this subsection, the dynamics of these circuits are linked to the electret potential, denoted by E in the rest of the letter. The value of the capacitance at the transducer's terminals is denoted by C_{var}.

Consider the transducer as a part of the circuit configurations HW1 or HW2, with C_{var} cyclically time-varying between maximum and minimum values (C_{max}, C_{min}), subsequently to a mechanical input excitation of the e-VEH

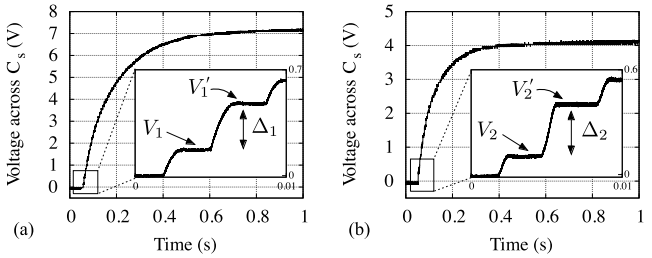

Fig. 2. Experimental measurement of $(\Delta_1, \Delta_2, V_1, V_2)$, measured on the MEMS electret transducer characterized in section III and reported in [10]. (a) Measured voltage across C_S with HW1 circuit. (b) Measured voltage across C_S with HW2 circuit.

(the same input for both circuit configurations). A cycle of variation of C_{var} is defined as its variation from C_{max} to C_{min} to C_{max}. The choice of the input is not constrained as long as it results in the same values C_{max} and C_{min} at each cycle. A harmonic input is used for simplicity. In the following, V_1 and V_2 denote the voltage across the fixed capacitor C_S at $C_{var} = C_{max}$ of a given variation cycle of C_{var}, for the HW1 and HW2 circuits respectively. The labels V_1' and V_2' denote the voltage across the fixed capacitor C_S at $C_{var} = C_{max}$ of the following cycle, for the HW1 and HW2 circuits respectively. We also define $\Delta_1 \coloneqq V_1' - V_1$ and $\Delta_2 \coloneqq V_2' - V_2$. The quantities (Δ_1, V_1) and (Δ_2, V_2) are measured on the time-evolution of the voltages across C_S with circuits HW1 and HW2, respectively. An experimental example of measurement of $(\Delta_1, \Delta_2, V_1, V_2)$ is shown in Fig. 2.

In the aforementioned input conditions, the electrical analysis of each circuit yields the cycle-to-cycle evolution law of the voltage across C_S, which reads:

$$V_1' = \frac{C_S V_1 + (C_{max} - C_{min})E - (C_{max} + C_{min})V_T}{C_{min} + C_S} \quad (1)$$

$$V_2' = \frac{C_S V_2 + (C_{max} - C_{min})E - (C_{max} + C_{min})V_T}{C_{max} + C_S} \quad (2)$$

where $V_T \geq 0$ denotes the fixed threshold voltage of the diodes, which are assumed to follow the ideal voltage-current diode law. From these two equations, it comes that the measured $(\Delta_1, \Delta_2, V_1, V_2)$ can be linked to E and C_{max} by:

$$C_{max} = \frac{C_S(\Delta_1 - \Delta_2) + C_{min}(\Delta_1 + V_1)}{\Delta_2 + V_2}, \quad (3)$$

$$E = \frac{(C_{min} + C_S)\Delta_1 + C_{min}V_1 + (C_{max} + C_{min})V_T}{C_{max} - C_{min}}. \quad (4)$$

The value of C_{min} can be measured by a synchronous detection method [12]. Note that in the case of interdigitated-combs transducer geometries, C_{min} is fixed independently of the harmonic input acceleration. Hence, it can be measured by traditional means of measurement of fixed capacitances.

B. Measurement Errors and Choice of the Circuit's Parameters

To measure E for a given transducer using (4), it is necessary to choose C_S, V_1, V_2, and the input acceleration. This subsection shows how these parameters have to be chosen in order to maximize the measurement accuracy.

In the following, δ_V denotes the uncertainty on the measured voltage across C_S due to the superposition of random error sources in a broad sense (e.g., thermal, reading amplifier, and quantization noises). Suppose that the uncertainty on V_T and C_{min} can be neglected, and that V_1 and V_2 are chosen to be approximatively equal to zero. The measurement uncertainties on E and C_{max} due to random errors are denoted by δC_{max} and δE, respectively. They are linked to δ_V following:

$$\frac{\delta_{C_{max}}}{C_{max}} = \delta_V \frac{\eta + \xi}{E\eta(\eta - 1)} \sqrt{(1+\xi)^2 + (\eta + \xi)^2} \quad (5)$$

$$\frac{\delta_E}{E} = \delta_V \frac{\sqrt{(\eta + \xi)^4 + (1+\xi)^4}}{E(\eta - 1)^2} \quad (6)$$

where $\xi \coloneqq C_S/C_{min}$ and $\eta \coloneqq C_{max}/C_{min}$.

From (5-6), it comes that the measurement uncertainty due to random error sources decreases by decreasing C_S. However, decreasing C_S increases the electromechanical coupling effect on the e-VEH's dynamics, thereby inducing a systematic measurement error on C_{max} and E. This is because equations (3-4) are derived from (1-2) assuming that (C_{max}, C_{min}) with circuit HW1 (in (1)) are equal to (C_{max}, C_{min}) with circuit HW2 (in (2)). But these circuits do not bias the transducer in the same way, and different biasing results in different electrostatic forces generated by each of the two circuits on the e-VEH's mobile mass. This, in turn, yields different mobile mass motions with each of the two circuits. Thus, in general, (C_{max}, C_{min}) with circuit HW1 cannot be considered equal to (C_{max}, C_{min}) with circuit HW2.

From the topologies of the circuits depicted in Fig. 1, it can be seen that the circuit HW1 biases the transducer with a voltage varying from E at $C_{var} = C_{max}$ to $E + V_1'$ at $C_{var} = C_{min}$. The circuit HW2 biases the transducer with a voltage varying from E at $C_{var} = C_{min}$ to $E - V_2'$ at $C_{var} = C_{max}$. By choosing C_S large and V_1, V_2 as small as possible, V_1', V_2' are small (see (1-2)). This ensures that the biasing of C_{var} throughout its variation is approximatively the same with both circuits (close to the voltage E). Therefore, increasing C_S reduces the systematic measurement error due to the differential impact of the electromechanical coupling.

The following procedure is proposed to choose C_S so as to reduce the measurement uncertainty due to random error sources, whilst ensuring that the systematic error due to the electromechanical coupling remains negligible. An admissible value for δ_E/E is decided a priori, and solving (6) for ξ gives the corresponding C_S. Note that this supposes an a priori estimation of η and E. The former can be measured by synchronous detection [12]. The latter can be estimated by one or several first inaccurate measurements (e.g., using an arbitrary value for C_S for the first measurement). The measurements are then carried out with this value of C_S. If C_{max} obtained from (3) is consistent with its value measured by synchronous detection, then E obtained from (4) using the same measured $(\Delta_1, \Delta_2, V_1, V_2)$ can be considered accurate. Otherwise, C_S that satisfies the desired δ_E/E margin results in a large systematic error on C_{max}, and hence on E. In this case, the measurement has to be carried out again with a larger C_S. The systematic error due to the electromechanical coupling will decrease, but the admissible uncertainties on E and C_{max} due to random error sources will increase.

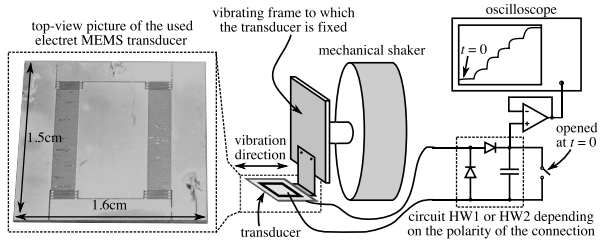

Fig. 3. Setup used for the measurement of the electret potential, with a top-view picture of the electret MEMS transducer. The device dimensions are $1.5\,\text{cm} \times 1.6\,\text{cm} \times 380\,\mu\text{m}$.

Finally, the measurement uncertainty can also be decreased by increasing η at fixed C_S. This is done by increasing the amplitude of the mechanical harmonic input. But as η results from the dynamics of the e-VEH's mechanical part, it is harder to use the input amplitude as a control parameter on the error.

Note that a technique employing the HW1 circuit has been used for electret potential measurement in [10], similar to the method presented in this letter, but using saturation voltages instead of local evolution voltages. Because of this, the method in [10] only holds if both C_{max} and C_{min} are fixed throughout the voltage evolution until saturation. This may not be verified because of the electromechanical coupling.

III. Experimental Results

In this section, the method is applied to a micro-scale electrostatic transducer realized in MEMS technology, similar to the device reported in [10]. The experimental setup is depicted in Fig. 3. As the transducer has an interdigitated-combs geometry, C_{min} is fixed, and C_{max} alternates between two different values at each period of the harmonic mechanical input excitation [10]. Therefore, there exists two values of C_{max} for each harmonic input that the device is submitted to. Two input are chosen: 1.5g and 2g amplitude, both of 150 Hz frequency.

In the setup used for this letter, the device is continuously submitted to the input vibrations, and C_S is first short circuited. Then, the short circuit is opened and the voltage evolution across C_S starts. But the time at which the short circuit is opened cannot be exactly chosen as corresponding to an extrema of C_{var}. To ensure that the captured evolution results from a complete cycle of variation of C_{var}, the first cycle of voltage evolution across C_S is ignored with both circuits. Hence, V_1, V_2 are slightly above zero (see Fig. 2).

To estimate the influence of random error sources on the measurement using (5-6), E is first estimated at 20 V, by a surface potential measurement done 1 mm on top of the device using a contact-less electrostatic voltmeter. The four values of η are measured by synchronous detection, and δ_V is measured as 25 mV. Using (6), the theoretical uncertainty on E decreases from 16.6% with the smallest C_{max}, to 4.2% with the largest C_{max}, all with $C_S = 100\,\text{pF}$.

These uncertainty intervals are satisfactory for this example, so the fixed capacitor is chosen as $C_S = 100\,\text{pF}$. Using an impedance-meter, C_{min} is measured as $C_{min} = 60\,\text{pF}$. The used diodes are JPAD5, whose parasitic capacitances values are negligible compared to C_S, and V_T is measured as $V_T = 0.7\,\text{V}$ for typical values of current in our application.

The results of the measurement method are depicted in Fig. 4. Each point corresponds to (E, C_{max}) obtained

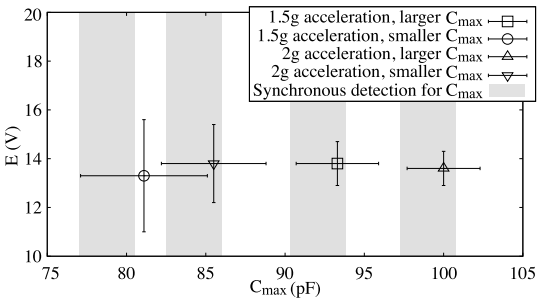

Fig. 4. Measurement results for E and C_{max}.

by averaging 5 measurements of $(\Delta_1, \Delta_2, V_1, V_2)$. The error bars represent the uncertainties obtained on $(\Delta_1, \Delta_2, V_1, V_2)$ propagated to (E, C_{max}). An example of a single measurement of $(\Delta_1, \Delta_2, V_1, V_2)$ obtained with the present device is depicted in Fig. 2. The results in Fig. 4 show that the obtained C_{max} are in accordance with those measured by synchronous detection. This guarantees that the systematic error due to the electromechanical coupling is negligible. As expected, the uncertainty on E decreases when the input amplitude increases (see end of Section II-B). Using the most accurate result, the electret potential is measured as $E = 13.7\,\text{V} \pm 5.1\%$. The uncertainty is slightly increased compared to the theoretical uncertainty obtained from (6), because of the lower effective value of E compared to its first estimation, and $V_1, V_2 > 0$.

For further validation, a voltage source of 5 V is added in series with the transducer to simulate a different value of the electret potential, and the measurement is carried out again. The expected electret potential is then of $E + 5$ by superposition. The used input is of 2g amplitude and 150 Hz frequency. The synchronous detection method gives $C_{max} = 102\,\text{pF} \pm 3\%$ (the lower value of C_{max} is discarded). From (6), keeping $C_S = 100\,\text{pF}$ results in an error of 3.3% on E. Using this value of C_S, the measurement yields a value of $E = 23.1\,\text{V} \pm 3.8\%$ and $C_{max} = 93\,\text{pF} \pm 3.1\%$. The value of C_{max} does not agree with what is measured by synchronous detection, which means that the systematic error due to the electromechanical coupling is large. Hence, the error minimization procedure discussed at the end of section II-B is applied: the admissible random error on E is relaxed to 7.5%, yielding $C_S = 180\,\text{pF}$. The new measurement gives $C_{max} = 103\,\text{pF} \pm 4.2\%$, which is in accordance with the value measured by synchronous detection. The electret potential is measured as $E = 19\,\text{V} \pm 6.8\%$, which is the expected value after adding the 5 V external voltage.

IV. Conclusion

This letter presented a method to accurately measure the value of the voltage source representing the electret in lumped parameter models of e-VEHs. The method was illustrated on an interdigitated-combs MEMS transducer, for which a traditional surface potential measurement across the transducer is hard to carry out and gives inaccurate results. The results were verified by comparing the maximum capacitance value, which is obtained as an intermediary parameter in the reported method, with its value measured by synchronous detection. The method was also validated by changing the charging conditions and checking the coherence of the results.

REFERENCES

[1] P. Pondrom, G. Sessler, J. Bös, and T. Melz, "Compact electret energy harvester with high power output," *Appl. Phys. Lett.*, vol. 109, no. 5, p. 053906, Aug. 2016, doi: 10.1063/1.4960480.

[2] Y. Suzuki, "Electret based vibration energy harvester for sensor network," in *Proc. 18th Int. Conf. Solid-State Sens. Actuators Microsyst. (TRANSDUCERS)*, Jun. 2015, pp. 43–46, doi: 10.1109/TRANSDUCERS.2015.7180856.

[3] D. Miki, Y. Suzuki, and N. Kasagi, "Effect of nonlinear external circuit on electrostatic damping force of micro electret generator," in *Proc. 15th Int. Solid-State Sens. Actuators Microsyst. Conf. (TRANSDUCERS)*, Jun. 2009, pp. 636–639, doi: 10.1109/SENSOR.2009.5285405.

[4] S. Boisseau, P. Gasnier, M. Gallardo, and G. Despesse, "Self-starting power management circuits for piezoelectric and electret-based electrostatic mechanical energy harvesters," *J. Phys., Conf. Ser.*, vol. 476, no. 1, p. 012080, 2013, doi: 10.1088/1742-6596/476/1/012080.

[5] J. Wei, E. Lefeuvre, H. Mathias, and F. Costa, "Interface circuit with adjustable bias voltage enabling maximum power point tracking of capacitive energy harvesting devices," *J. Micromech. Microeng.*, vol. 26, no. 12, p. 124008, 2016, doi: 10.1088/0960-1317/26/12/124008.

[6] A. Karami, D. Galayko, and P. Basset, "Series-parallel charge pump conditioning circuits for electrostatic kinetic energy harvesting," *IEEE Trans. Circuits Syst. I, Reg. Papers*, vol. 64, no. 1, pp. 227–240, Jan. 2017, doi: 10.1109/TCSI.2016.2603064.

[7] S. Boisseau, G. Despesse, and B. A. Seddik, "Electrostatic conversion for vibration energy harvesting," in *Proc. Small-Scale Energy Harvesting*, 2012, pp. 91–134.

[8] P. Basset, E. Blokhina, and D. Galayko, *Electrostatic Kinetic Energy Harvesting*. Hoboken, NJ, USA: Wiley, 2016.

[9] S. Boisseau, J. J. Chaillout, J. S. Danel, J. B. Legras, and G. Despesse, "Stable DRIE-patterned SiO2/Si3N4 electrets," in *Proc. 17th Int. Conf. Solid-State Sens. Actuators Microsyst. (Transducers Eurosensors XXVII)*, Jun. 2013, pp. 1942–1945, doi: 10.1109/Transducers.2013.6627174.

[10] Y. Lu, E. O'Riordan, F. Cottone, S. Boisseau, D. Galayko, E. Blokhina, F. Marty, and P. Basset, "A batch-fabricated electret-biased wideband MEMS vibration energy harvester with frequency-up conversion behavior powering a uhf wireless sensor node," *J. Micromech. Microeng.*, vol. 26, no. 12, p. 124004, Sep. 2016, doi: 10.1088/0960-1317/26/12/124004.

[11] M. Renaud, G. Altena, R. Elfrink, M. Goedbloed, C. De Nooijer, and R. Van Schaijk, "Modeling and characterization of electret based vibration energy harvesters in slot-effect configuration," *Smart Mater. Struct.*, vol. 24, no. 8, p. 085023, Jul. 2015, doi: 10.1088/0964-1726/24/8/085023.

[12] P. Basset, D. Galayko, A. M. Paracha, F. Marty, A. Dudka, and T. Bourouina, "A batch-fabricated and electret-free silicon electrostatic vibration energy harvester," *J. Micromech. Microeng.*, vol. 19, no. 11, p. 115025, 2009, doi: 10.1088/0960-1317/19/11/115025.